XMM-Newton observation of distant, energetic pulsar J2022+3842

Prakash Arumugasamy[1], George Pavlov[1], Oleg Kargaltsev[2]
[1]Department of Astronomy and Astrophysics, Pennsylvania State University, 525 Davey Lab., University Park, PA 16802, USA
[2]Department of Physics, The George Washington University, Washington, DC 20052, USA

1 Introduction

PSR J2022+3842 is a young ($\tau \approx 8.9$ kyr) and energetic pulsar at a distance of ~ 10 kpc located in the center of SNR G76.9+1.0 discovered by Arzoumanian et al. (2011).
It was claimed to be the fastest and second most energetic non-recycled pulsar in our Galaxy after a 24 ms period detection in the radio (GBT) and X-rays (RXTE).

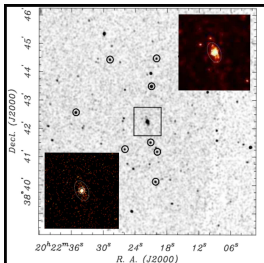

Fig. 1.1 : Chandra ACIS-S3 0.5 – 7 keV X-ray image of G76.9+1.0 center. 1° X 1° region around PSR J2022+3842 insets showing un-smoothed and smoothed PSR+PWN. Arzoumanian et. al (2011)

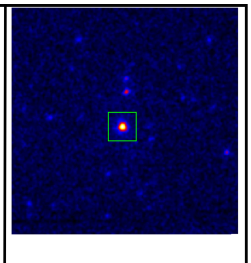

Fig. 1.2 : XMM-Newton EPIC MOS1 0.5 - 12 keV smoothed image, 8′ X 10′ around PSR J2022+3842. 1′ X 1′ window in green.

A 54 ks *Chandra* observation had shown no SNR emission, a weak yet distinct pulsar wind nebula (PWN) and a low spin-down power to X-ray conversion efficiency.

$$F^{\rm abs}_{\rm PWN}/F^{\rm abs}_{\rm PSR}\ (2-10\ {\rm keV}) \approx 0.08$$

$$\eta_{X,0.5-8{\rm keV}} = L_{X,0.5-8{\rm keV}}/\dot{E} = 5.5\times10^{-5} D^2_{10}$$

We perform spectral analysis of pulsed and off-pulsed emission using data from a longer XMM-*Newton* observation to better understand the X-ray properties of the pulsar.

Observation : 110 ks XMM-*Newton* observation. EPIC-pn & MOS2 operated in timing mode offer time resolution of 0.03 ms and 1.5 ms respectively, retaining position information in 1 dimension. Target imaged only in MOS1 (Fig. 1.1).

2 Data Analysis

MOS1 data used to locate and characterize nearby point sources in the field that contaminate pn data.

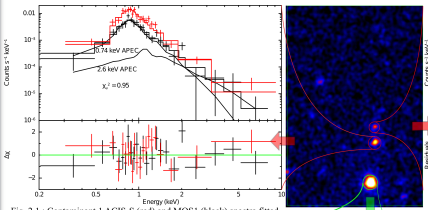

Fig. 2.1 : Contaminant 1 ACIS-S (red) and MOS1 (black) spectra fitted with two APEC components, their chi-sq. residuals (bottom panel)

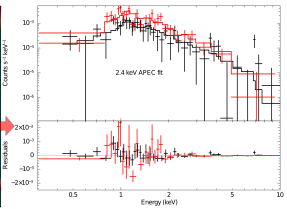

Fig. 2.2 : Contaminant 2 ACIS-S (red) and MOS1 (black) spectra fitted with single component APEC model, their C-stat. residuals (lower panel).

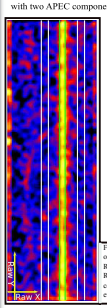

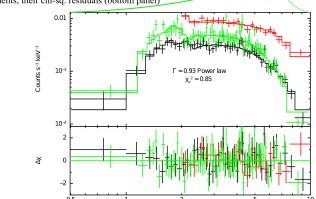

Fig. 2.3 : PSR J2022+3842 phase integrated ACIS-S (black), MOS1 (green) and pn (red) spectra fitted with absorbed power law model and the chi-sq. residuals.

Fig. : EPIC-pn timing mode data visualised with one dimensional event positions along CCD Raw X coordinate and time of arrival along Raw Y. Fast readout achieved by collapsing columns along CCD Raw Y and reading out the events' Raw X and time values.

2.1 Contaminant analysis

APEC models emission spectrum from collisionally ionized diffuse gas.
Early-type stars are known to exhibit such spectrum (Getman et al. 2006). Contaminant 1 is coincident with HD 194094, a B0V star in cluster.
The two contaminants' spectra peak below 1 keV and rapidly decline above 2 keV. In pn, the contaminant sources have projected separation of $\sim 9''$ (2 pixels) from pulsar position.

2.2 Timing Analysis

We detect unambiguous 48 ms pulsations in the EPIC-pn timing data, twice the previously reported value. Z^2_4 periodicity test shows significant contribution from ≥ 20 harmonics.
The X-ray pulse profile shows two, narrow ($\Delta\phi \approx 0.09$) peaks (Main pulse and Inter-pulse), phase separated by $\Delta\phi = 0.48$ with $> 77\%$ pulsed fraction.
A glitch of magnitude $\Delta\nu/\nu = 2.2\times10^{-7}$ is likely to have occured between MJD 55227 - MJD 55666.

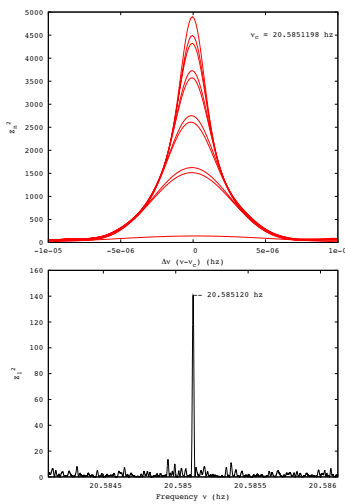

Fig. 3 : Pulsar rotation frequency search using Z^2_1 test (Bottom); Z^2_4 values around the central frequency value of 20.5851198 hz for harmonics 1 - 10.

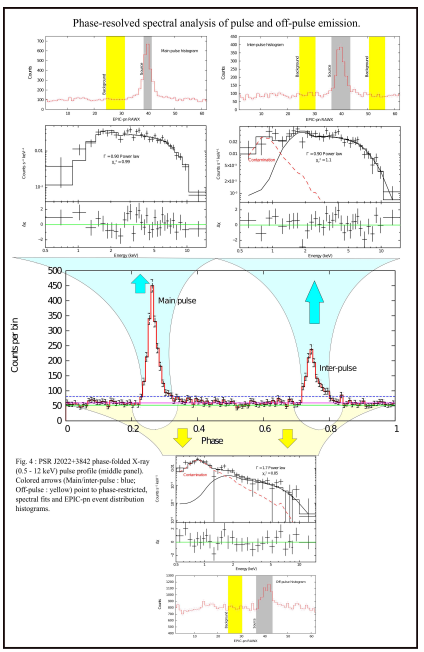

Fig. 4 : PSR J2022+3842 phase-folded X-ray (0.5 - 12 keV) pulse profile (middle panel). Colored arrows (Main/inter-pulse : blue; Off-pulse : yellow) point to phase-restricted, spectral fits and EPIC-pn event distribution histograms.

Table 1: Best fit parameter values with 90% confidence limits for various pusiar phases.

	N_H (10^{22} cm^{-2})	Γ	PL. norm.[a]	χ^2/d.o.f.	$F^{\rm abs}_{0.5-10{\rm keV}}$[b]	$F^{\rm unabs}_{0.5-10{\rm keV}}$[b]
Integrated	$2.32^{+0.29}_{-0.26}$	$0.93^{+0.10}_{-0.09}$	$4.53^{+0.84}_{-0.68}$	0.85/138	$6.17^{+0.25}_{-0.25}$	$7.62^{+0.27}_{-0.26}$
Main pulse	$2.23^{+0.67}_{-0.56}$	$0.90^{+0.19}_{-0.17}$	$17.7^{+6.82}_{-4.71}$	0.99/29	$25.7^{+1.6}_{-1.6}$	$31.4^{+2.5}_{-2.2}$
Inter-pulse	2.32 (Fixed)	$0.90^{+0.13}_{-0.14}$	$12.8^{+2.74}_{-2.44}$	1.10/31	$18.5^{+1.5}_{-1.5}$	$22.7^{+1.6}_{-1.6}$
Off-pulse	2.32 (Fixed)	$1.70^{+0.76}_{-0.71}$	$2.29^{+2.55}_{-1.41}$	0.85/28	$0.89^{+0.38}_{-0.34}$	$1.44^{+0.42}_{-0.40}$

[a] Power law normalisation in units of 10^{-5} photons cm^{-2} s^{-1} keV^{-1} at 1 keV.
[b] $F^{\rm abs}_{0.5-10{\rm keV}}$ & $F^{\rm unabs}_{0.5-10{\rm keV}}$ are the absorbed and unabsorbed, average (over respective phase range) flux in units of 10^{-13} erg cm^{-2} s^{-1}.

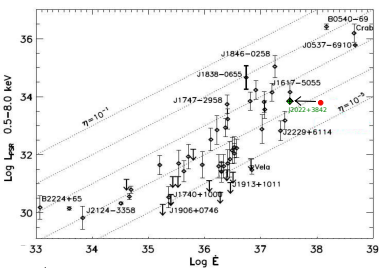

Fig. 5 : X-ray luminosity of pulsar versus spin-down power. The old (red dot) and new (green diamond) position for J2022 +3842 on the plot are shown.

3 Conclusions

1. Pulsar J2022+3842's true rotation period is 48 ms and spin-down power $\dot{E} = 2.96\times10^{37}$erg s^{-1}cm^{-2}. Not the fastest rotator or second most energetic young pulsar.
2. Hard ($\Gamma \approx 0.9$) pulsed emission and softer ($\Gamma = 1.7$) off-pulse emission. PWN contribution in the off-pulse phase might be significant.
3. X-ray efficiency $\eta_{X,0.5-8{\rm keV}} \approx 2.4\times10^{-4}$, close to efficiencies of similar young pulsars.
4. No SNR emission detected in the 110 ks XMM observation. Soft SNR emission likely extinguished in the high N_H inter-stellar medium.